Use of a linear continuous reference electrode to monitor the chloride-induced corrosion of steel in prestressed concrete

M. Ormellese*, A. Brenna and L. Lazzari

(Received: August 27, 2013)
(Accepted: September 26, 2013)

1 Introduction

Post-tensioning tendons contribute decisively to the safety, serviceability and durability of pre-stressed concrete structures, especially in the case of highway and railways viaducts and bridges. To enhance durability, optimum corrosion protection of tendons has been a priority since the introduction of this technology. Nevertheless failures of pre-stressing and post-tensioning steel, mainly induced by chlorides penetration, are well known in the civil engineering field [1].

The critical aspects of durability are summarized in a state of the art report [2,3]: main problems are related to localised corrosion due to the penetration of chloride-containing water in concrete. Pitting corrosion of high strength steel is very harmful since it leads to brittle failures due to hydrogen embrittlement mechanism. As localised corrosion of passive steel starts when chloride concentration exceeds a critical threshold (about 600 ppm by concrete weight) at steel surface, at the pit tip an acid condition sets up producing hydrogen atom and promoting hydrogen embrittlement on susceptible steels.

For these reasons in the last two decades more attention was paid in establishing technical specifications, selecting materials, for instance the use of drawing steel instead of quenched and tempered steels, defining design strategies, especially to build new post-tensioned concrete structures [4,5]. About durability, the principle of a multi-task protection is adopted to prevent chlorides penetration: the use of adequate drainage systems, waterproofing coatings and structural detailing are some examples. In addition the importance of a reliable monitoring system has been underlined [2,3,6,7]. NDT techniques were described, such as acoustic emission, ultrasonic and magnetic methods, able to detect defects in the plastic ducts, grout voids and non-perfect tendon encapsulation. Instead, there is no established electrochemical method for monitoring the localised corrosion of internal steel strands. Since hydrogen embrittlement is a consequence of pitting corrosion, being not possible to directly monitor the hydrogen embrittlement phenomenon, a good strategy would be to monitor pitting initiation through the monitoring of the steel free corrosion potential. Also the technique based on the check of the insulation between tendon and metallic sheath is used, through the monitoring of the integrity of the sheath regardless the starting of corrosion [8].

Potential mapping is the only widely recognized and standardized non-destructive technique for assessing and locating areas of corrosion on steel rebars in concrete structures. In addition to the American Standard ASTM C876 [9], a RILEM recommendation has been published [10], where the extensive recent experience with potential mapping has been included. Several national guidelines describe the use and interpretation of half-cell potential measurements. For normal reinforced concrete structures exposed to atmosphere, such as viaducts or bridges, the potential mapping permits to identify the corroding areas: the initiation of chloride-induced corrosion is detected by a drop of

M. Ormellese, A. Brenna, L. Lazzari
Dipartimento di Chimica, Materiali e Ingegneria Chimica "G. Natta" – Politecnico di Milano, Via Mancinelli, 7 20131, Milano (Italy)
E-mail: marco.ormellese@polimi.it

the rebar free corrosion potential to more negative with respect to the typical free corrosion potential in passive condition. According to ASTM C876 [9], when rebar potential is higher than −200 mV CSE the probability of corrosion is very low, whereas if the rebar free corrosion potential is lower than −350 mV CSE the probability of corrosion is very high.

In the case of encapsulated tendons, the steel potential cannot be measured by means of a portable reference electrode, since tendons are practically isolated from the external environment being encased in metallic or plastic ducts. To measure the potential, fixed reference electrodes should be embedded within the duct and the measured potential is representative of the corrosion condition taking place nearby. To monitor the potential of the whole metallic structures several fixed reference electrodes have to be installed, but this is very expensive and impossible to achieve in real structures.

To overcome the problem, in 1995 *Wietek* proposed the use of a linear continuous reference electrode (LCRE), claiming that, once a pit occurs in any position on the steel, the potential measured by the LCRE drops to values typical of active range, giving promptly the evidence of pitting occurrence [11]. This new conception reference electrode consists of a silver/silver chloride reference electrode wire to be wrapped along the whole length of the tendon inside the duct.

From the practical point of view, the use of such a LCRE is very appealing because of the simplicity. Nevertheless, concerns on the true meaning of the potential reading in practical applications arose both from theoretical point of view and because of lack of similar use in electrochemistry. It is well know that, in the presence of a macrocell, for example in the case of a localised corrosion attack, there is a current flowing from the anodic site (the pit) to the cathodic surfaces, then establishing within the electrolyte a potential gradient or, in other words, a set of equipotential surfaces. When using a standard local portable reference electrode, the measured potential is the one of the equipotential surface crossed by the electrode; moving from the pit to the cathodic surface the potential reading increases from negative values to more positive ones. If a wire-type reference electrode is used, several equipotential surfaces are crossed, then mismatching the meaning of the potential reading.

Then laboratory tests were performed on a wire-type reference electrode in order to verify the ability to detect the initiation of localised corrosion and to understand the meaning of the potential reading.

2 Materials and methods

Test cell assembly was designed to simulate the electric field established by pitting corrosion of carbon steel tendon embedded in alkaline mortar within a plastic duct, such as in pre-stressed concrete structures.

For the sake of simplicity, a small cylindrical cell (60 mm in diameter and 0.6 m length) was used (Fig. 1). To simulate the concrete resistivity and the length of a real duct (some meters long) the cell was filled with distilled water (pH 6.5, resistivity 150 Ω m). The passive condition of carbon steel in alkaline mortar was simulated using a AISI 304 stainless steel rod (10 mm in diameter), which is very passive in neutral solution. It is well-known in fact that the corrosion behaviour of carbon steel in concrete is the same of stainless steel in neutral solution [1].

To control the initiation of a localised corrosion attack, an inert anode was placed into the cell; the anode supplied a constant current by means of an external galvanostat feeding unit. The anode was placed both in the middle of the stainless steel rod, to have a symmetric electric field, and at one end. A constant 1 mA current was supplied by the anode in order to have on the cathodic surface (the stainless steel rod) a current density in the range 50–70 mA/m^2, very close to the real cathodic current densities measured on real tendons encased in plastic ducts.

It is fundamental to underline that the electric field trend obtained with the designed impressed current system is the same as the one established by a real pitting macrocell, except the anode potential value. Indeed, in a real pitting macrocell, anode potential of the pit is about −0.7 V SCE (i.e. the potential of the corroding area of the iron falls on the active behaviour) and cathodic zone

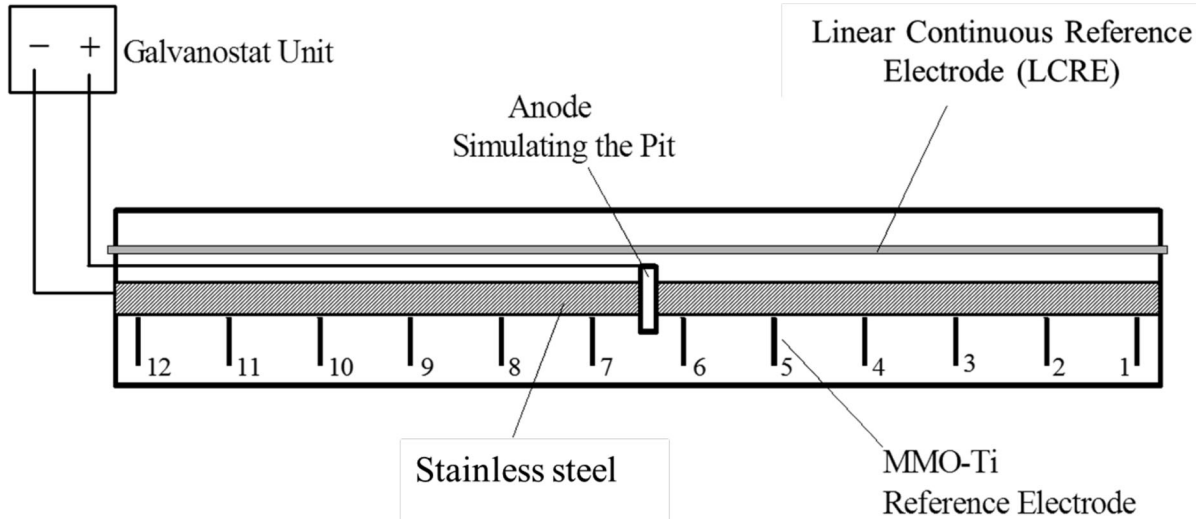

Figure 1. Schematic representation of the cell used for laboratory tests on LCRE

Table 1. Series of performed laboratory tests

Series	MMO-Ti		LCRE	Position of the simulated localized corrosion attack	Cycle steps
1	12	Separated Short-circuited	–	Central position, Lateral position	5 (see Table 2)
2	2	Separated Short-circuited	–	Central position, Lateral position	5 (see Table 2)
3		–	1	End	3

potential is more positive, close to −0.2 V and −0.5 V SCE [1]; instead, in an impressed current system, even if the anode potential is more positive than the cathode, the potential distribution on the cathodic zone is the same as in a real pitting macrocell.

To measure and monitor the potential profile on the cathodic surface of the stainless steel rod, 12 separated activated titanium reference electrodes (titanium coated with mixed metal oxide, MMO-Ti RE) were placed all along the rebar, with 50 mm spacing (Fig. 1). The electrodes were placed as close as possible to the rebar in order to minimize the ohmic drop contribution. An activated titanium wire (1 mm in diameter) was used as LCRE and placed 10 mm from the stainless steel rod. The stability of the electrodes was continuously checked by an external saturated calomel electrode (SCE) through a Luggin capillary.

Three series of tests were performed (Table 1):

- series 1: tests with 12 MMO-Ti REs, through two conditions: one taking the reference electrodes separated and the second condition by short-circuiting the reference electrode in order to simulate a LCRE. The aim of this series of measurements was to verify the capability of the electrodes to detect the occurrence of a localised corrosion
- series 2: tests using only 2 MMO-Ti REs, under the same previous conditions, i.e. separated or short-circuited, in order to verify the stability of the reference electrodes and their polarization
- series 3: tests with a LCRE.

Tests of series 1 and 2 were carried out by following a five-step cycle, as reported in Table 2. In series 3, a three-step cycle was performed: first step without applied current (no pitting, passive condition only), second step by setting up a macrocell simulating the presence of a localised corrosion, and then last step after switching the macrocell current off.

3 Results

Figure 2 reports the stainless steel rod potential measured by means of the 12 MMO-Ti REs, under the five-step cycle test (Table 2). Two condition were tested: localised corrosion attack located in centre of the rod (position No. 6 of the cell in Fig. 1) and at one end (position No. 2 of the cell in Fig. 1). During step 1 (absence of a macrocell, i.e. passive condition), free corrosion potential of the stainless steel rod is almost constant, close to −0.3 mV versus MMO-Ti (Fig. 2a). During step 2, with a macrocell current of 1 mA, a clear profile was measured: in position No. 6, i.e. close to the anode, potential lowered to −2.5 V versus MMO-Ti, then indicating that a cathodic current entered the stainless steel rod, while in adjacent positions No. 5 and No. 7 MMO-Ti RE cathodic polarization was lower, then fading on farther positions. When MMO-Ti reference electrodes were short-circuited to simulate a LCRE (step 3), the potential reading was −1.3 V versus MMO-Ti. On step 4, after current was switched off, steel potential grew up to −0.3 V versus MMO-Ti, close to values measured in step 1, indicating passive condition.

Figure 2b shows potential measurements with the anode placed in the end position of the stainless steel rod (position No. 2 of the cell in Fig. 1). During step 1 (absence of macrocell current), potential measured by the 12 separated reference electrodes was close to 0 V versus MMO-Ti, more positive than the previous test. This value was attributed to the higher presence of oxygen in the cell. During step 2, electrodes were short circuited to simulate a

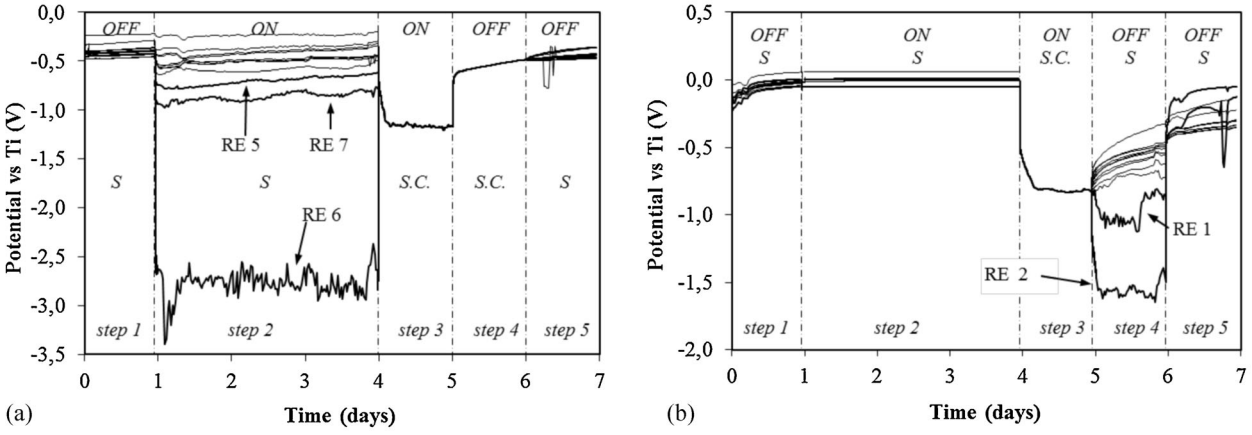

Figure 2. Stainless steel rod potential profile measured with the 12 MMO-Ti reference electrodes: (a) artificial anode in central position, (b) artificial anode in end position. Applied current 1 mA

Table 2. Typical cycle for tests of series 1 and 2

Step	1	2	3	4	5
Current	OFF	OFF	ON	ON	ON	OFF	OFF
Simulated pit	No	No	Yes	Yes	Yes	No	No
Electrodes[a)]	S	S.C.	S	S.C.	S	S.C.	S

[a)]S – separated; S.C. – short circuited.

LCRE: no potential variation was observed. Then a macrocell current of 1 mA was supplied to simulate the localised corrosion attack (step 3): the simulated LCRE measured a drop of potential to −0.8 V vs MMO-Ti. According to step 4, all the 12 MMO-Ti REs were separated: as expected potential measured with MMO-Ti RE No. 2 (facing the inert anode) showed the lowest value, about −1.6 V versus MMO-Ti. After the current switching off (step 5), stainless steel potential measured by the 12 reference electrodes grew up to values in the range of −0.3 V and 0 V versus MMO-Ti.

A second series of tests was performed using only two short circuited MMO-Ti REs. Results are reported in Fig. 3. The anode was placed in the centre of the stainless steel rod (position No. 6, Fig. 1). Two condition were considered: (a) reference electrodes in symmetric position (electrodes No. 5 and No. 7 of Fig. 1); (b) reference electrodes in non-symmetric position with respect to the anode (electrodes No. 4 and No. 6 of Fig. 1). In the absence of a macrocell current (step 1) potential of the stainless steel rod was close to −0.1 V/−0.2 V versus MMO-Ti, then indicating passive condition. After 1 mA macrocell current was supplied (step 2), rebar potential in both cases (symmetric and non-symmetric) lowered to about −0.5 to −0.7 V versus MMO-Ti, where the more negative potential was measured by the reference electrode closer to the inert anode.

After short circuiting (step 3) stainless steel potential remained almost constant, about −0.6 V versus MMO-Ti. The current was then switched off, to re-establish passive condition: rebar potential increased up to −0.1/−0.2 V versus MMO-Ti.

Figure 4 reports MMO-Ti REs potential measurements performed with an external SCE reference electrode placed close to the MMO-Ti REs by means of a Luggin capillary (Fig. 1). Tests were carried out to check possible interference of the short-circuited reference electrodes. In the absence of macrocell current (passive condition) with separated electrodes (step 1), MMO-Ti reference electrodes potential was in the range of +0.12 V and +0.20 V versus SCE. After current application (step 2), no significant potential variation was measured on the separated electrodes. Then electrodes were short circuited (step 3). Considering reference electrodes in symmetrical position with respect the simulated localized corrosion attack (Fig. 4a) a negligible potential variation was measured, lower than 20 mV. In the case of non-symmetrical condition (Fig. 4b) the potential of the MMO-Ti RE close to the simulated corrosion attack decreased in the cathodic direction of more than 50 mV, whereas the potential of the other MMO-Ti REs, far away from the localised corrosion attack, increased in the anodic direction of more than 50 mV (Fig. 4b). Those variations vanished after current switch off (steps 4–5).

To confirm the anodic and cathodic potential variation of the short circuited MMO-Ti REs, tests were carried out simulating a non-symmetric electrical field by placing the simulated corrosion attack in end position (No. 11, Fig. 1). The two electrodes in position No. 11 and No. 4 were considered. Results are reported in Fig. 5. As previously demonstrated, in the presence of an induced localised corrosion attack (macrocell current on, step 2), stainless steel rod potential close to the inert anode decreased to −2.0 V versus MMO-Ti (Fig. 5a), whereas stainless steel rod potential far away from the anode decreased less than 100 mV (indicating that this part of the rod is not affected by the induced macrocell. The so negative measured potential (−2.0 V versus MMO-Ti) should not mislead: even if in a real pit situation a potential as negative as

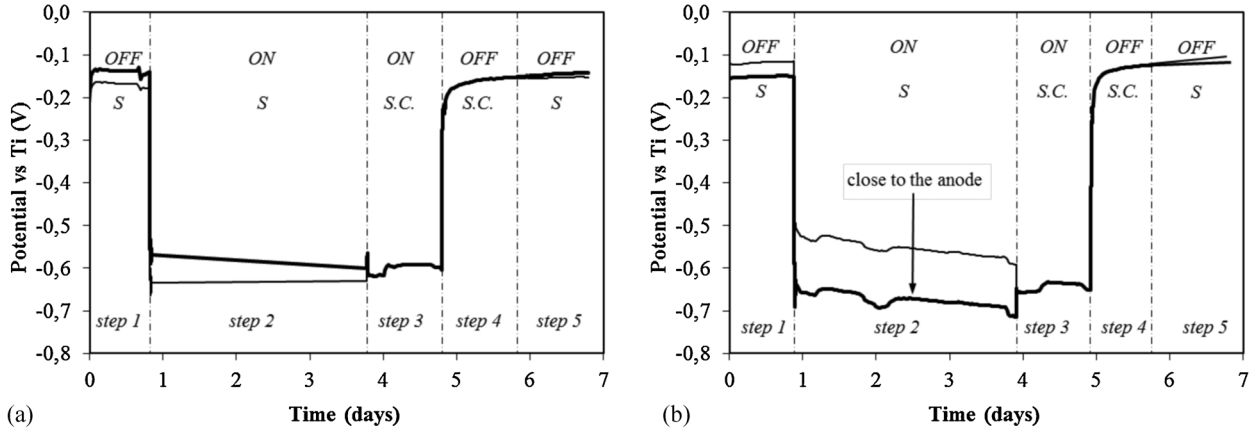

Figure 3. Stainless steel rod potential profile measured by short circuiting two MMO-Ti REs in the presence of a localized corrosion attack in center position: (a) electrodes symmetrically placed with respect to the inert anode; (b) electrodes not symmetrically placed with respect to the inert anode

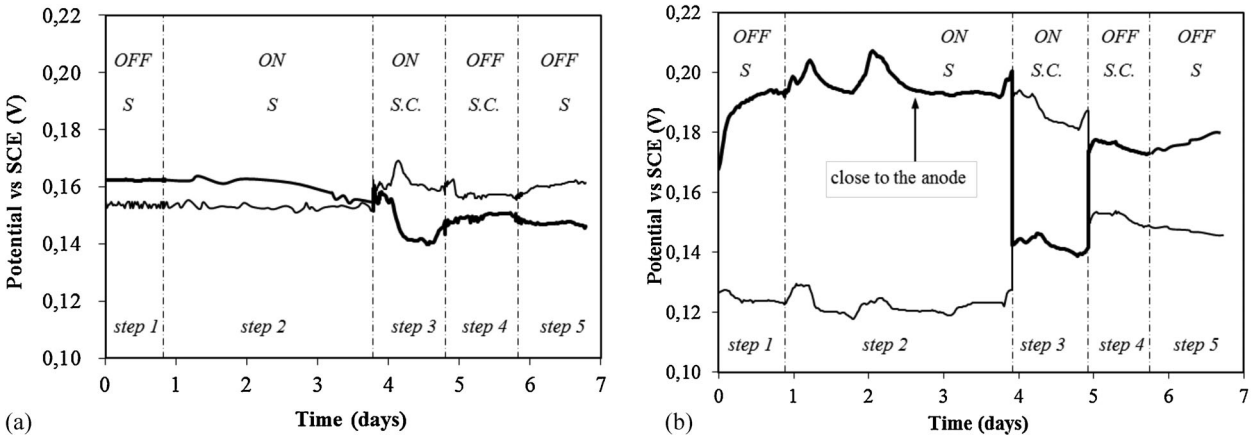

Figure 4. Potential profile of the two MMO-Ti REs measured with external SCE in the presence of a localized corrosion attack in center position: (a) electrodes symmetrically placed with respect to the inert anode; (b) electrodes not symmetrically placed with respect to the inert anode

−0.7 V is expected, in the simulated pit due to the very high local current density on the rod facing the inert anode, so negative potentials are possible. After short circuiting the two electrodes (step 3), the measured rebar potential was −1.2 V versus MMO-Ti (Fig. 5a), increasing to −0.3 V versus MMO-Ti once current was switched off (step 4).

Potentials of the two MMO-Ti REs were monitored through external SCE (Fig. 5b). Considering step 3 (electrodes short circuited to simulate a LCRE, macrocell current on to simulate a pit), it was confirmed that the potential of the reference electrode close to the inert anode lowered towards the cathodic direction, from +0.4 V versus SCE to −0.1 V versus SCE, whereas the potential of the reference electrode far away from the anode increased in the anodic direction, from +0.3 to +1.0 V versus SCE.

The same test was then performed considering all the 12 reference electrodes, with the simulated localized corrosion attack in end position No. 11. Stainless steel potential profile and the potential of the 12 MMO-Ti REs were monitored. Figure 6a shows the rod potential trend. As in previous tests, in step 1 rod potential was close to −0.3 V versus MMO-Ti RE; after current application the stainless steel potential near the anode lowered, while no variations were observed in the area far away from the simulated corrosion attack (step 2). After electrode short circuiting (step 3), stainless steel potential reading became −1.0 V versus MMO-Ti.

Polarization of the 12 MMO-Ti REs is shown in Fig. 6b. Initially, the 12 MMO-Ti REs were separated; their free corrosion potential ranged from +0.2 to +0.4 V versus SCE. No potential variation was observed after the switch on of the current simulating the localised corrosion (step 2). After electrodes short circuiting (step 3), potential measured at the MMO-Ti RE No. 11 close to the anode, decreased in the cathodic direction from +0.4 V vs SCE to −0.3 V vs SCE, while potential of all the other electrodes increased up to +0.8 V versus SCE; only MMO-Ti RE No. 9 (the nearest to MMO-Ti RE No. 11) showed a lower potential increase to about +0.6 V versus SCE.

In the third test series, a linear wire-type reference electrode was used (LCRE); the localised corrosion attack was simulated by placing the inert anode in end position No. 11 (Fig. 1). Figure 7a shows stainless steel rod potential profile measured by means of the external SCE through Luggin capillaries to eliminate ohmic drop contribution in the readings. Potential was +0.1 V SCE in

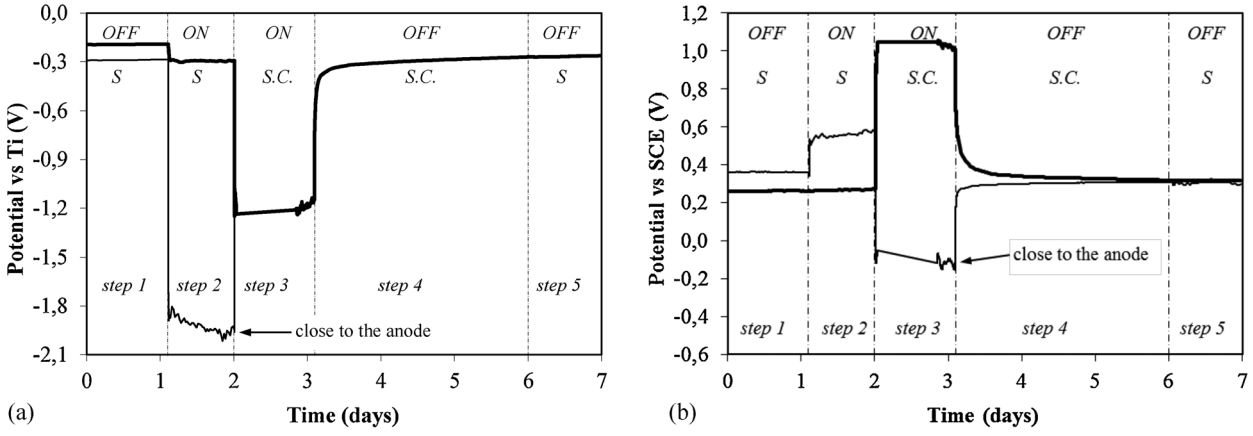

Figure 5. Potential profile in the presence of a localized corrosion attack placed in end position: (a) stainless steel rod potential with respect to two internal MMO-Ti RE; (b) MMO-Ti RE potential with respect to external SCE

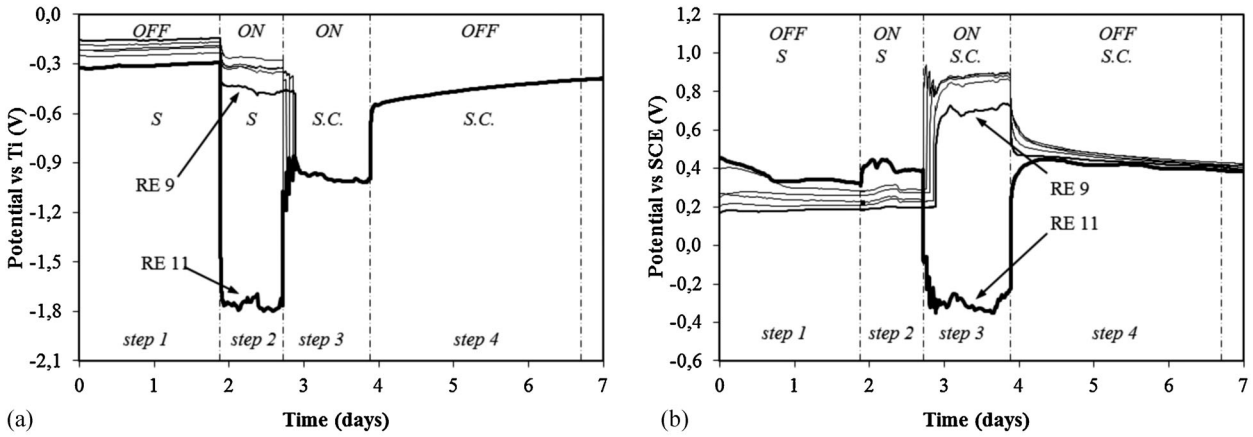

Figure 6. Potential profile in the presence of a localize corrosion attack placed in end position: (a) stainless steel potential with respect to the 12 MMO-Ti REs; (b) MMO-Ti REs potential with respect to the external SCE

the first step (passive condition); then, after macrocell current application (step 2), potential decreased to −1.2 V versus SCE if measured close to the anodic site, and remained almost constant to −0.2 V versus SCE if measured in the other positions. Stainless steel rod potential was also measured with the LCRE (Fig. 7b): in passive condition (step 1) potential was −0.25 V versus LCRE; in active condition (macrocell current on) the potential decreased to −0.9 V versus LCRE (step 2). Figure 7c reports the potential profile of the LCRE carried out by means of six SCE placed all along the LCRE as close as possible to it to eliminate the ohmic drop contribution. As previously observed with the short circuited MMO-Ti REs, in the presence of a pit, a cathodic polarization was observed in the area close to the anode, while an anodic polarization was measured in the area far from the anode.

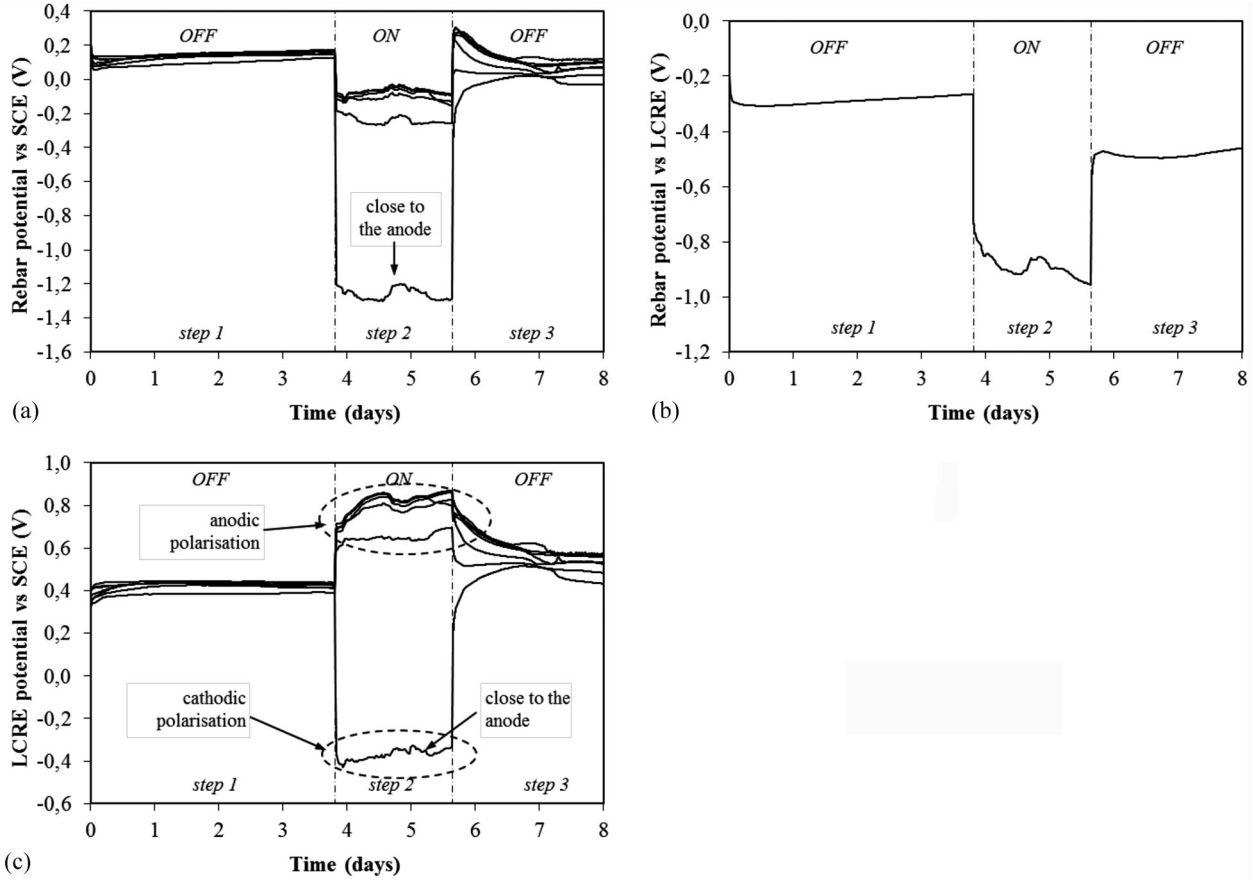

Figure 7. Laboratory test in the presence of a LCRE: (a) stainless steel potential with respect to external SCE; (b) stainless steel potential with respect to LCRE; (c) LCRE potential with respect to external SCE

4 Discussion

Laboratory tests were performed to study the ability of a linear wire-type continuous reference electrode (LCRE) to monitor the potential of a carbon steel tendon encased in a plastic duct filled with alkaline concrete. Tests were performed simulating the electric field occurring once a pit is initiated. Results are hereafter discussed highlighting three main aspects: (1) the ability of a LCRE to detect the initiation of chloride-induced corrosion; (2) the meaning of a potential reading by means of a wire-type electrode; (3) the use of the LCRE on real structures.

4.1 Ability of a LCRE to detect the initiation of chloride-induced corrosion

Potential measurement is a useful technique to detect the set up of a chloride-induced corrosion on carbon steel rebar in concrete. The reading is simply performed by connecting to a voltmeter a reference electrode and the metallic structure that has to be monitored, by placing the reference electrode in contact with the same electrolyte of the structure.

To detect the occurrence of localised corrosion in concrete, criteria suggested in ASTM C876 [9] may be considered: initiation of corrosion is highly probable if the rebar free corrosion potential lowers more than 200 mV with respect to the typical values of passive condition.

As a consequence, potential readings performed with the separated MMO-Ti REs, with the short-circuited reference electrodes and with the LCRE may be analysed taking into account that a potential reduction is an indication of a localized corrosion initiation.

Figure 8 summarises potential profile measured on the stainless steel rod by means of the 12 separated MMO-Ti REs and after their short circuiting to simulate a LCRE. Profiles were obtained both in the absence and in the presence of an artificial localised corrosion attack located in the centre of the rod (Fig. 8a) and at one end (Fig. 8b). In passive condition (macrocell current off) potential of separated and short circuited electrodes is similar, −0.3 V versus MMO-Ti and −0.1 V versus MMO-Ti in the case of central and lateral simulated localised corrosion, respectively; the potential difference is determined by the different oxygen availability. In the presence of an impressed macrocell current applied to simulate the pit, the 12 separated reference electrodes gave the typical potential profile in the presence of a initiated localised corrosion attack: more negative potential close to the pit, less negative potential far away from it (Fig. 8). As previously stated, the so negative measured potential (about −3.0 V versus MMO-Ti) should not mislead: even if in a real pit situation a potential as negative as −0.7 V is expected, in the simulated pit, due to the very high local current density on the surface of the rod facing the inert anode, so negative potentials are possible. The measured potential profiles confirmed the presence of an artificial induced pit.

Also the 12 short circuited MMO-Ti REs, simulating the LCRE, were able to detect the initiation of corrosion; in fact when active conditions were established (external current on), the measured steel potential diminished from −0.1/−0.3 V versus MMO-Ti towards more negative values, about −1.2 V versus MMO-Ti (Fig. 8a). The same can be stated for tests performed in the presence of a localised corrosion attack at one end of the steel rod (Fig. 8b).

Tests directly performed with a LCRE confirm its ability to detect the initiation of corrosion. Taking into account Fig. 7b, the stainless steel potential reading given by the LCRE was −0.25 V versus MMO-Ti and −0.90 V versus MMO-Ti in the absence (passive condition) and the presence (pitting condition) of the macrocell current, respectively.

For the adopted geometry, the LCRE gave the clear and promptly indication of the presence of the pitting macrocell, since a significant drop of potential was detected.

As specified in the materials and methods section, laboratory tests were performed on a stainless steel rod placed in a cylindrical cell filled with distilled water in order to simulate a carbon steel tendon encased in plastic ducts filled with concrete. This approach is valid since the corrosion behaviour of carbon steel in concrete is the same of stainless steel in neutral solution [1]. In any case the ability of LCRE has to be verified on a geometry similar to real conditions.

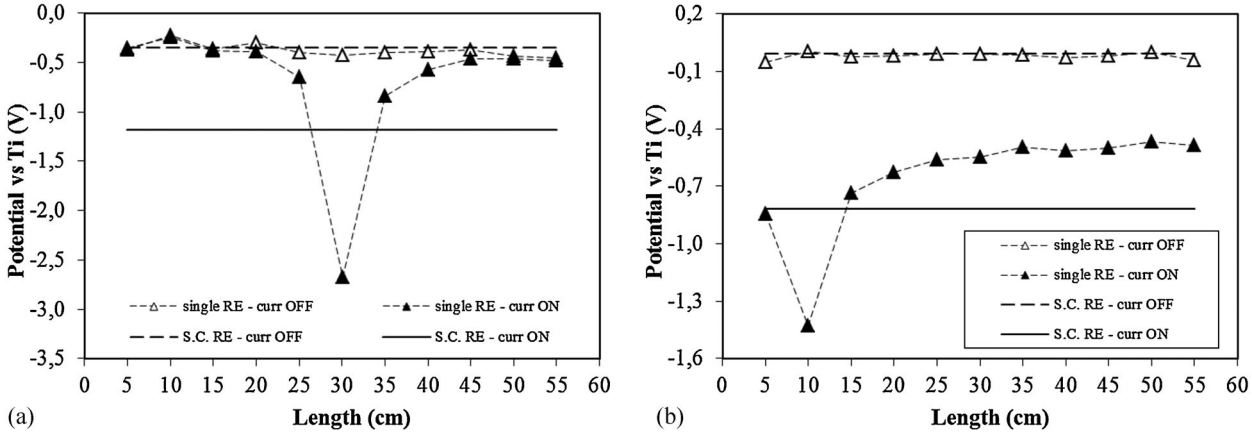

Figure 8. Stainless steel potential profile with respect to the short circuited and separated MMO-Ti reference electrodes: (a) inert anode in central position; (b) inert anode in end position

4.2 Meaning of a potential reading with wire-type reference electrode

To interpret the meaning of the potential reading performed with a linear continuous metallic wire such as a LCRE the following has to be considered: when a metallic wire is crossing an electrical field (the one produced by the presence of a localised corrosion attack) it contributes to the current flow because of its electrical conductivity. In other words, the LCRE behaves as an interfered metallic wire immersed in an electrical field established by the pitting macrocell; according to this, some zones of the LCRE become cathodic, where the current enters the wire, and some others become anodic, where the current leaves it. This behaviour has already been observed in an application of cathodic protection of a concrete bridge with activated Ti mesh anode when current was off and chlorides were present [12].

The voltage drop within the LCRE is the same established in the environment by the macrocell current between the anode (the pit) and the cathode (surrounding steel surfaces). As clearly reported in Figs. 5–7c, experimental results confirmed the interfering condition occurring on a real LCRE as well as on a simulated LCRE. Same results are reported in Fig. 9 where LCRE potential was measured by means of six external SCEs: in the absence of a localised corrosion attack (current off) the LCRE potential profile is about +0.19 V versus SCE; when an artificial pitting corrosion attack is simulated, the LCRE potential measured by means of external SCE lowered in the area close to the corrosion attack (the LCRE is cathodically interfered, then a current enters the wire), whereas the potential increased far away for the localised corrosion attack (the LCRE is anodically interfered, then a current leaves the wire).

Taking into account the electrical scheme when measuring the potential between the corroding steel and the LCRE, considering that the steel is affected by a potential profile which depends on the macrocell current set up by the localised attack (more negative values located close to the anodic site) and the LCRE is electrically interfered by an electrical field established by the localised attack, the stainless steel potential reading performed with the LCRE can only be the result of the potential profiles established by the macrocell current and measured by Lugging probe on both the rebar and the LCRE.

Based on the these assumptions, the stainless steel potential measured by using the LCRE could be estimated as the difference between the weighted potential profile of the rebar and the weighted potential profile of the LCRE, both measured by means of the external not interfered SCE reference electrodes. A similar approach has been reported in ref. [13] to interpret the pipe-to-soil potential of a coated pipeline buried in soil in the presence of some defects with different polarization level.

The weighted average potential, $E_{electrode}$, is calculated as follow:

$$E_{electrode} = \sum_i S_i E_i / \sum_i S_i \tag{1}$$

where S_i is the surface having potential E_i. The surface S_i may be estimated as follow

$$S_i = \pi \cdot \Phi \cdot L_i \tag{2}$$

where Φ is the rod diameter and L_i the portion of the rod having potential E_i.Eq. (1) then shortens to the following;

$$E_{electrode} = \sum_i L_i E_i / \sum_i L_i \tag{3}$$

On the basis of Eq. (1), the stainless steel rod potential readings performed by means of a LCRE may be calculated as follow:

$$E_{SS}^{LCRE} = E_{SS}^{LCRE} - E_{LCRE}^{SCE} = \frac{\sum_i L_i^{SS} E_i^{SS}}{\sum_i L_i^{SS}} - \frac{\sum_i L_i^{LCRE} E_i^{LCRE}}{\sum_i L_i^{LCRE}} \tag{4}$$

where L_i is length of the stainless steel rod (or of the LCRE) having a potential E_i.

Considering the stainless steel and LCRE potential profiles in the presence of a localised corrosion attack (Fig. 10), sectioning

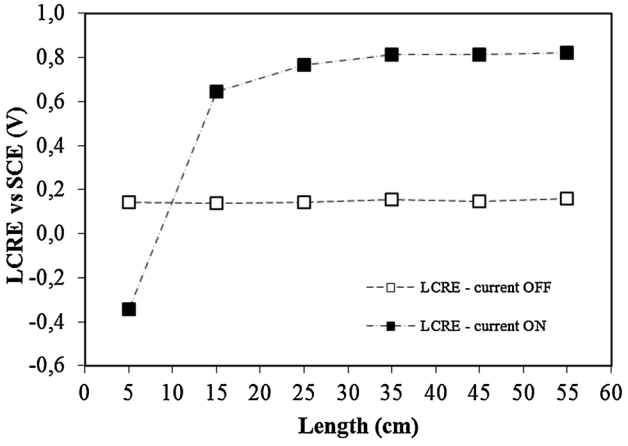

Figure 9. LCRE potential profile with respect to external SCE in passive condition and in the presence of a localized corrosion attack in end position

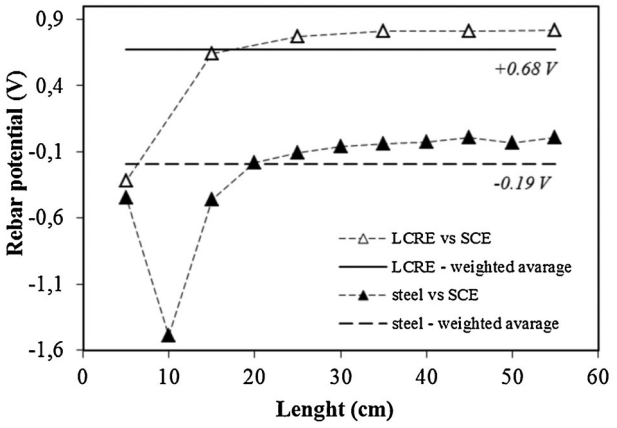

Figure 10. LCRE and stainless steel potential profile and weighted average values in the presence of a localized corrosion attack in end position

the 600 mm long stainless steel rod in some pieces of length L_i, each one with a potential E_i, the rebar weighted potential is -0.19 V versus SCE and the LCRE weighted potential is $+0.68$ V versus SCE. Applying Eq. (4), the rebar potential should be the difference between the two weighted values, equal to -0.87 V versus LCRE. The potential of the steel rod experimentally measured with respect to the LCRE is -0.90 V (Fig. 7b), then confirming the hypothesized meaning of a potential reading by means of a continuous wire reference electrode.

4.3 Possible use of the LCRE on real structures

Based on the found relationship (Eq. 4), some doubts arose on the efficiency of a LCRE to detect a localised corrosion attack when used for long structures, above all if a little localised corrosion attack is coupled with an extended cathodic passive area.

In a localised corrosion attack the equipotential surface distribution is determined by the so-called throwing power of the macrocell induced by the pit [14]. The latter permits to evaluate the maximum distance at which the anodic current, flowing from the pit, is absorbed by the cathodic surface; in other words, the throwing power permits to estimate the extension of the cathodic surface involved in the corrosion process.

A rough evaluation of the throwing power, L, inside a duct can be obtained by solving the Ohm's laws, assuming the presence of a uniform current density, i, taking into account the driving force, ΔV, that produced the pit (the difference between the potential at the anodic and the cathodic site), the electrolyte resistivity, ρ, and the duct diameter, ϕ. The following equation may be derived [14]:

$$L = \sqrt{\frac{2 \cdot \Delta V \cdot \phi}{\rho \cdot i}} \tag{5}$$

Considering a driving force in the range of 0.5–0.6 V (typical value for pitting corrosion), the average diameter of a duct in the range of 10–20 cm, the resistivity of concrete in the range of 100–200 Ω m and the current density lower than 20 mA/m^2 (due to the limited availability of oxygen), the throwing power ranges from 0.5–1.1 m. Obviously it is limited by the low conductivity of the concrete and the diameter of the polymeric duct.

As a direct consequence, the interfering effect on the LCRE is limited, and then its ability to detect the localised corrosion attack. The surfaces of the tendons and the LCRE far away from the area involved in the corrosion process are not influenced by the pit presence, working at a constant equipotential value typical of passive condition. For examples, taking into consideration a LCRE 10 m long, being the pitting corrosion initiation clearly detected only if a potential drop of at least 0.2 V is measured with respect to the passive condition (as reported in ASTM C876 [9]), in the presence of a pit, whose influence is in the range of a meter, the average potential detected by the LCRE approximates the one of the unaffected surface areas in passive condition, which are prevailing. Then the LCRE electrode wouldn't be able to detect the localised corrosion occurrence. LCRE is properly working only in the case of short tendons. As a first approximation it is possible to assume a maximum length of 5 m.

Based on the experimental results, a newly conceive reference electrode for pitting corrosion monitoring of pre-stressed and post-tensioned concrete structure was proposed and developed [15], consisting of a series of multiple successive wire-type reference electrodes to be placed all along the tendons with a proper length in relation to the geometry of the structure (mainly the cover) and the concrete, or grout, resistivity. Some preliminary laboratory results were presented somewhere [16].

5 Conclusions

A wire-type LCRE has been proposed to detect localised corrosion occurrence on carbon steel tendons encased in polymeric or metallic ducts in pre-stressed or post-tensioned concrete structures. Concerns on the true meaning of the potential reading in practical applications using a wire-type reference electrode arose both from theoretical point of view and because of lack of similar use in electrochemistry. Since no literature data are available, a series of lab tests has been planned and performed. Results allow to state the following:

- the LCRE is able to detect the occurrence of pitting corrosion, provided the length of the monitored tendons is in the order of few meters
- the LCRE, once pitting started, behaves as an interfered electrode immersed in an electrical field; some zones of the electrode becomes cathodic and others anodic
- the potential reading can be interpreted as the difference of the potential averages, weighted on equipotential surface areas, of the steel and the LCRE
- based on the mechanism of the potential reading, the LCRE is not efficient in detecting the localised corrosion attack if used for long structures, since potential of areas unaffected by pitting macrocell (passive steel) prevail with respect to the pitting surface
- a new conception reference electrode for pitting corrosion monitoring of pre-stressed and post-tensioned concrete structure was proposed and developed consisting of a series of wire-type reference electrode, each one maximum few meters long.

6 References

[1] L. Bertolini, B. Elsener, P. Pedeferri, R. Polder, *Corrosion of Steel in Concrete*, 1st Edn., Wiley-VCH, Weinheim **2004**.

[2] *Durability of post-tensioning tendons*, FIB Technical Report Bulletin 15, Edited by Luc Taerwe, International Federation for Structural Concrete FIB, Lausanne, Switzerland **2001**.

[3] *Durability specifics for pre-stressed concrete structures: durability of post-tensioning tendons*, FIB TG 5.4.2, Commission 15, Structural Service Life Aspects **2004**.

[4] M. Perrin, L. Gaillet, C. Tessier, H. Idrissi, *Corros. Sci.* **2010**, *52*, 1915.

[5] J. Sánchez, J. Fullea, C. Andrade, J. J. Gaitero, A. Porro, *Corros. Sci.* **2008**, *50*, 1820.

[6] S. Feliu, J. A. González, J. M. Miranda, V. Feliu, *Corros. Sci.* **2005**, *47*, 217.

[7] P. Montes-García, F. Castellanos, J. A. Vásquez-Feijo, *Corros. Sci.* **2010**, *52*, 555.
[8] J. Ayats, A. Gnagi, B. Elsener, *Proc. Int. FIB Congress*, Prestressed Concrete Engineering Association, Vol. 6, Session 8, 2002 169–176, Osaka, Japan.
[9] ASTM C876, *Standard test method for half-cell potential on reinforcing steel in concrete*, American Society for Testing and Materials, West Conshohocken, PA 19428-2959, United States, **2009**.
[10] B. Elsener, C. Andrade, J. Gulikers, R. Polder, M. Rapauch, *Mater. Struct.* **2003**, *36*, 461.
[11] B. Wietek, US Patent 5,403,550, **1995**.
[12] L. Bertolini, P. Pedeferri, T. Pastore, B. Bazzoni, L. Lazzari, *Corrosion* **1996**, *52*, 552.
[13] T. J. Barlo, R. R. Fessler, presented at *Int. Conf. Corrosion/83*, NACE International, Houston, TX, paper 292, **1983**.
[14] L. Lazzari, P. Pedeferri, *Cathodic Protection*, 1st Edn., Polipress, Milan, Italy **2006**.
[15] L. Lazzari, P. Pedeferri, M. Ormellese, *European Patent Application N. 05718514.2*, **2005**.
[16] L. Lazzari, M. Ormellese, P. Pedeferri, presented at *Int. Conf. Corrosion NACE*, NACE International, Houston, TX, Paper 05372, **2005**.